SAND2000-0669J

Growth of compaction bands: a new deformation mode for porous rock

William A. Olsson and David J. Holcomb

Sandia National Laboratories, Albuquerque, NM

Abstract

Compaction bands are thin, tabular zones of grain breakage and reduced porosity that are found in sandstones. These structures may form due to tectonic stresses or as a result of local stresses induced during production of fluids from wells, resulting in barriers to fluid (oil, gas, water) movement in sandstone reservoirs. To gain insight into the formation of compaction bands we have produced them in the laboratory. Acoustic emission locations were used to define and track the thickness of compaction bands throughout the stress history during axisymmetric compression experiments. Narrow zones of intense acoustic emission, demarcating the boundaries between the uncompacted and compacted regions were found to develop. Unexpectedly, these boundaries moved at velocities related to the fractional porosity reduction across the boundary and to the imposed specimen shortening rate. Thus compaction bands were found to grow in the direction of maximum compression stress. This appears to be a previously unrecognized, fundamental mode of deformation of a porous, granular material subjected to compressive loading with significant implications for the production of hydrocarbons.

Geologists and rock mechanicians have long recognized fracture (discontinuous) and flow (continuous) as two modes of inelastic deformation of rocks subjected to all-around compressive stresses [1]. The fractures that form when the compressive shear strength limit has been reached are called shear fractures or faults. These fractures occur in planes of high shear stress oriented at an acute angle to the direction of maximum compressive stress and are characterized by significant relative tangential offset of the fracture walls. Deformation by flow can result in various patterns of strain depending on conditions of temperature, pressure, and deformation rate. Mechanical flow can take place by frictional, brittle or crystal plastic

DISCLAIMER

DISCLAIMER

Portions of this document may be illegible in electronic image products. Images are produced from the best available original document.

mechanisms. For much of the history of experimental rock deformation, the rocks studied were of relatively low porosity such as granites, marbles and quartzites. In these materials shear fracture is often accompanied by dilatancy (inelastic volume expansion resulting from nucleation and propagation of microcracks) [2] of the material and the nascent fracture zone. Compactive deformation has appeared to be relatively uniform in the few studies of porous rocks where compaction played any significant role [3, 4]. Mollema and Antonellini [5] described a type of geological structure called a compaction band that showed that natural compaction has sometimes been nonuniform. These bands are tabular features of a millimeter or two in thickness and up to tens of meters in length that are characterized by predominantly compactive deformation. It was noticed recently [6] that some laboratory features in porous rock [7, 8, 9] and even in honeycomb structures [10] had similar descriptions. The structures described in [7], [8] and [9] were associated with cylindrical holes intended to model the full-scale operation of oil and gas well drilling and tunneling. In these studies slot-like features resulted from crushing of the material in a tabular zone that extended from the hole and were oriented normal to the local maximum compression. In the case of formation during drilling under compressive boundary loads with flushing water, the features were empty slots.

Olsson [6] applied a strain localization theory [11] and performed axisymmetric, confined compression experiments on Castlegate sandstone (a quartz granulate with 28% porosity) in an attempt to reproduce compaction bands in the laboratory. The strain localization theory predicted the appearance of compaction bands for certain values of constitutive parameters that were consistent with the measured values of Castlegate sandstone. Features similar to compaction bands did form in the specimens, but they were thicker (approximately 2.5 cm) than those observed in the rock outcrops. The experiments described in this report were undertaken to gain further insight into the compaction process and to shed light on the differences between the bands observed in the field and those formed in the laboratory.

All tests were conducted under axisymmetric loading conditions, consisting of an increasing compressive load applied along the axis of a cylindrical rock specimen while a constant pressure was maintained on the sealed cylindrical surface by a fluid pressure medium. Specimens of Castlegate sandstone, a commonly-used analog of reservoir rock, were cored parallel

to bedding, sawed and ground into right-circular cylinders with diameter 50.8 mm and length 127 mm. Cores were taken parallel to bedding to eliminate the possibility of lithological variations influencing the results. Tested specimens were air-dry and vented to the atmosphere. The cylinders were covered with a 0.127-mm thick copper foil to which 14 ultrasonic transducers were attached. A urethane coating was applied over the foil to prevent intrusion of the liquid confining medium (Isopar) into the specimen. Hardened steel end caps of matching diameter were attached at each end of the sample to match the sample diameter to the somewhat larger diameter of the loading piston (see Figure 1).

Because of the low elastic modulus of the Castlegate sandstone, frictional end constraints are significant where the steel end caps press against the cylinder ends during loading along the cylinder axis. Prior experiments had shown that the normal practice of placing the steel end caps directly against the rock surface resulted in high stress gradients with associated anomalous deformation and concentrations of acoustic emissions at the interface, even using the best available lubrication to reduce friction. A sucessful technique to reduce the end effects consisted of placing a copper cap over the rock cylinder end and molybdenum disulphide lubricant and Teflon tape on the end of the loading piston. As discussed later, this arrangement eliminated the stress concentration at one end.

During a given test, the confining pressure was first raised to the desired level, then the axial deformation was induced by advancing the loading piston at a displacement rate of 5.8×10^{-4} mm/sec. Sample deformations were measured using LVDTs (linear variable differential transformers) parallel and perpendicular to the sample axis giving ϵ_{11} (axial) and ϵ_{33} (lateral) strains, respectively. These are engineering strains defined as change in length divided by original length. Acoustic emissions were recorded throughout the experiment using a full wave form, 32 MHz recording system to capture the signals from the 14 piezoelectric transducers. Each AE event is assumed to correspond to one of the grain-scale events, such as grain cracking or grain boundary slip, that are the microscopic source of the inelastic macroscopic compaction of the sample. Events were located post-test with techniques similar to those used in seismology for locating earthquakes; locations were triangulated based on the arrival time differences for the compressional elastic waves generated by each event using an

automated routine for determining arrival times and a simplex algorithm for locating events. During the course of a typical experiment, several million discrete events were observed, of which a random 1% or fewer were recorded for later location, with the percentage determined by the 5 event/second recording rate of the AE system. Location accuracies were estimated to be ± 3 mm.

The axial stress difference, σ_D (axial stress minus confining pressure), plotted against axial strain, ϵ_{11}, for the specimen discussed here is shown in Fig. 2. The curve is characterized by 4 segments. First is the steeply rising linear segment indicating largely elastic behavior, up to about $\sigma_D = 65$ MPa (Region I, Fig. 2). Second, is the small peak where the stress drops about 5 MPa below the yield stress at 90 MPa (II, Fig. 2) to the third segment, the constant stress region that extends to about 6.5% strain (III, Fig. 2). The fourth segment begining at 6.5% strain indicates a strengthening of the rock (IV, Fig. 2). All specimens that showed compaction banding had this specific overall shape.

Acoustic emission events (AE) have been associated with microcracking [1] and, in particular with grain breakage associated with pore collapse in sandstones [13]. The locations of about 1% of the AE were determined, allowing the microcracking activity to be traced throughout the test history. Our results for one experiment are exhibited in Figure 3, which consists of 16 panels representing the AE activity during successive stages of the experiment, reading from left to right. Each panel contains two views of the located AE events projected onto orthogonal planes parallel to the sample axis, with the boundary of the sample shown as a heavy box and each event represented by a dot. In addition, each panel plots the differential stress (σ_D) as a function of the strain parallel to the loading axis (ϵ_{11}) for the entire test (same data as Fig. 2), with a highlighted region indicating the portion of the test represented by the AE locations. Thus Figure 3 can be seen as 16 frames of a movie showing the evolution of the AE activity as the sample was compacted.

As expected the AE were fairly uniformly distributed during hydrostatic compression by the liquid confining medium (not shown). There was, however, intense AE activity concentrated in a tabular zone at the steel end cap/specimen interface at the beginning of the differential loading phase (Panel 1, Fig. 3). The other end of this specimen was separated

from the steel by a copper sheet and layer of lubricant composed of 50:50 stearic acid and petroleum jelly between the copper and the steel endcap. There was no concentration of AE at that end suggesting that this greatly reduces the shear stress on the end of the specimen.

Shortly after differential loading began, the AE concentration at the lower end of the sample disappeared and the distribution of events became uniform (Panel 2,3, Fig. 3), remaining uniform until the peak stress was attained. Coincident with yielding, the peak in the stress-strain curve, a new AE zone appeared, displaced upward from the interface (Panel 5, Fig. 3), began to move toward the center of the specimen with increasing specimen shortening. The AE zone moved uniformly with shortening from just after yield until about 8% shortening. Then, in Panel 9, a second zone began to form near the top end of the specimen, coincident with a slight increase in load. This top zone began to move downward in panels 14 and 15. Near 8% shortening, the two zones of AE collide (Panel 15), whereupon AE activity essentially ceased and the stress began to rise slowly. This curve is typical of curves for specimens that showed compaction banding.

Animations of both the AE distribution, shown in Fig. 3 and AE density profiles plotted versus specimen length show definitely that the zones of intense microcracking activity formed at or near the yield stress and moved with increasing axial shortening at a rate that was proportional to the constant axial displacement rate being applied to the end of the specimen. When the zones meet, the AE rates drops to nearly zero.

The maxima on a plot of AE density versus axial position were used to compute the velocity of the movement of AE zone(s) across the specimen; an example for a specimen that exhibited two zones that started simultaneously, one at each end, is shown in Figure 4. The net velocity shown in Figure 4 is 4.8×10^{-3} mm/s compared to the applied shortening rate of 5.8×10^{-4} mm/s. These numbers are equivalent to those for the specimen of Figure 4.

Our results concerning the formation of compaction bands and their growth, demonstrate that we have discovered a new mode of deformation of porous rock, and possibly porous granulates, in general. In the experimental setup that we used, compaction bands nucleated in high stress gradient zones near interfaces. As the axial stress was increased above hydrostatic the distribution of AE became uniform until peak stress, whereupon new band(s) appeared

displaced inward a short distance from the interfaces, and then propagated (thickened) in a direction parallel to the direction of maximum compressive stress. The propagation of the band front (or fronts) continued completely through the length of the specimen until all material has been compacted. An analysis completely analogous to the problem of a shock wave moving through a material undergoing a phase change [14] is consistent with all measured parameters and features of the quasistatic, axisymmetric, confined compression experiments. This calculation predicts that the porosity drops from 28 to 18% across the band front. Observational work in progress finds that the porosity in the compacted zone is of the order of 18% [15].

Porosity is reduced and intense grain breakage occurs during the compaction banding process which is expected to occur naturally when stresses become sufficiently large or to be induced by human activities such as withdrawal of fluids from porous formations, i.e. oil and gas production. The formation of compaction bands is likely to reduce permeability, creating a barrier to fluid flow. Also the grain breakage and microstructural weakening could lead to the borehole breakout phenomena described by Haimson and Song [9] and Bessinger et al. [8] causing increased sand production in oil wells. Impeding fluid flow and increasing sand production would have significant economic consequences for the petroleum industry. The relationship of the laboratory compaction bands to those observed in the field has not been fully established. It is clear that the driving mechanism for the bands we observed in our experiments was the continuing applied shortening. Possibly, in a large body of rock, a smaller amount of shortening interacts with an initial distribution of strength defects to cause a distribution of thin bands.

References

[1] M. S. Paterson, *Experimental Rock Deformation–The Brittle Field*, (Springer-Verlag, New York, 1978).

[2] W. F. Brace, B. W. Paulding, C. Scholz, *J. Geophys. Res.* **71**, 3939 (1966).

[3] T.-F. Wong, H. Szeto, J. Zhang, *Appl. Mech. Rev.* **45**, 281 (1992).

[4] T.-F. Wong, C. David, W. Zhu, *J. Geophys. Res.* **102**, 3009 (1997).

[5] P. N. Mollema, M. A. Antonellini, *Tectonophysics* **267**, 209 (1996).

[6] W. A. Olsson, *J. Geophys. Res.* **104**, 7219 (1999).

[7] E. Z. Lajtai, *Int. J. Fract.* **10**, 525 (1974).

[8] B. A. Bessinger, Z. Liu, N. G. W. Cook, L. R. Myer, *Geophys. Res. Lett.* **24** (1997).

[9] B. C. Haimson and I. Song, *SPE/ISRM Rock Mechanics in Petroleum Engineering*, Soc. Petrol. Eng., Richardson, Tex. (1998).

[10] S.D. Papka, S. Kyriakides, *Int. J. Solids Struct.* **36**, 4367 (1999).

[11] J. W. Rudnicki, J. R. Rice, *J. Mech. Phys. Solids* **23**, 371 (1975).

[12] K. A. Issen, W. Rudnicki, submitted *J. Geophys. Res.*, (1999).

[13] J. Zhang, T.-F. Wong, D. M. Davis, *J. Geophys Res.* **95**, 341 (1990).

[14] W. A. Olsson, Quasistatic shock waves: a growth mechanism for compaction bands in porous granulates, unpublished manuscript.

[15] J. T. Fredrich, A. DiGiovanni, D.J. Holcomb and W.A. Olsson, *Accepted by North American Rock Mech. Symp., August 2000*

[16] Supported by the U.S. Department of Energy's Office of Basic Energy Sciences/Geosciences and the Office of National Petroleum Technology. Sandia is a multiprogram laboratory operated by Sandia Corporation, a Lockheed Martin Company, for the U.S. Department of Energy under contract DE-ACOC4-94AL85000.

Figure 1: Photograph of sample showing ultrasonic transducers (pins protruding from sides of sample), copper and urethane coating and steel end caps.

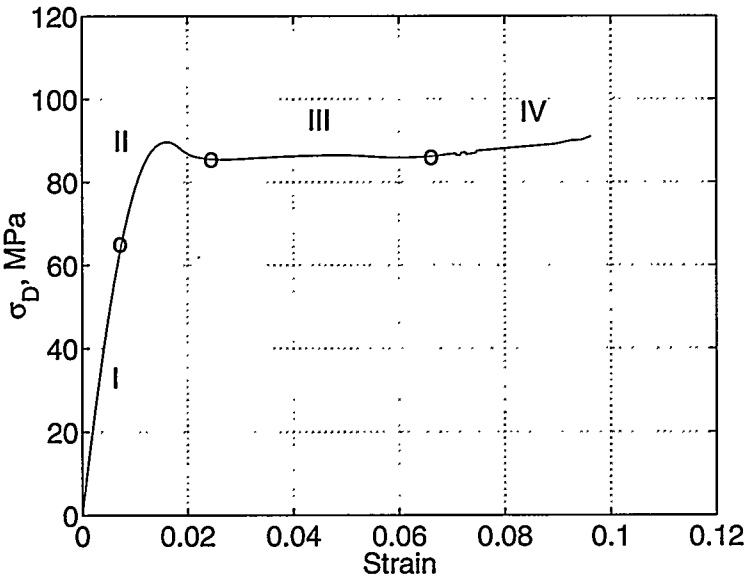

Figure 2: Differential stress, σ_D, plotted against fractional shortening, ϵ_{11}, for a specimen of Castlegate sandstone that underwent compaction banding. Regions separated by o's and labelled I, II, III, and IV are discussed in text. Confining pressure was 45 MPa.

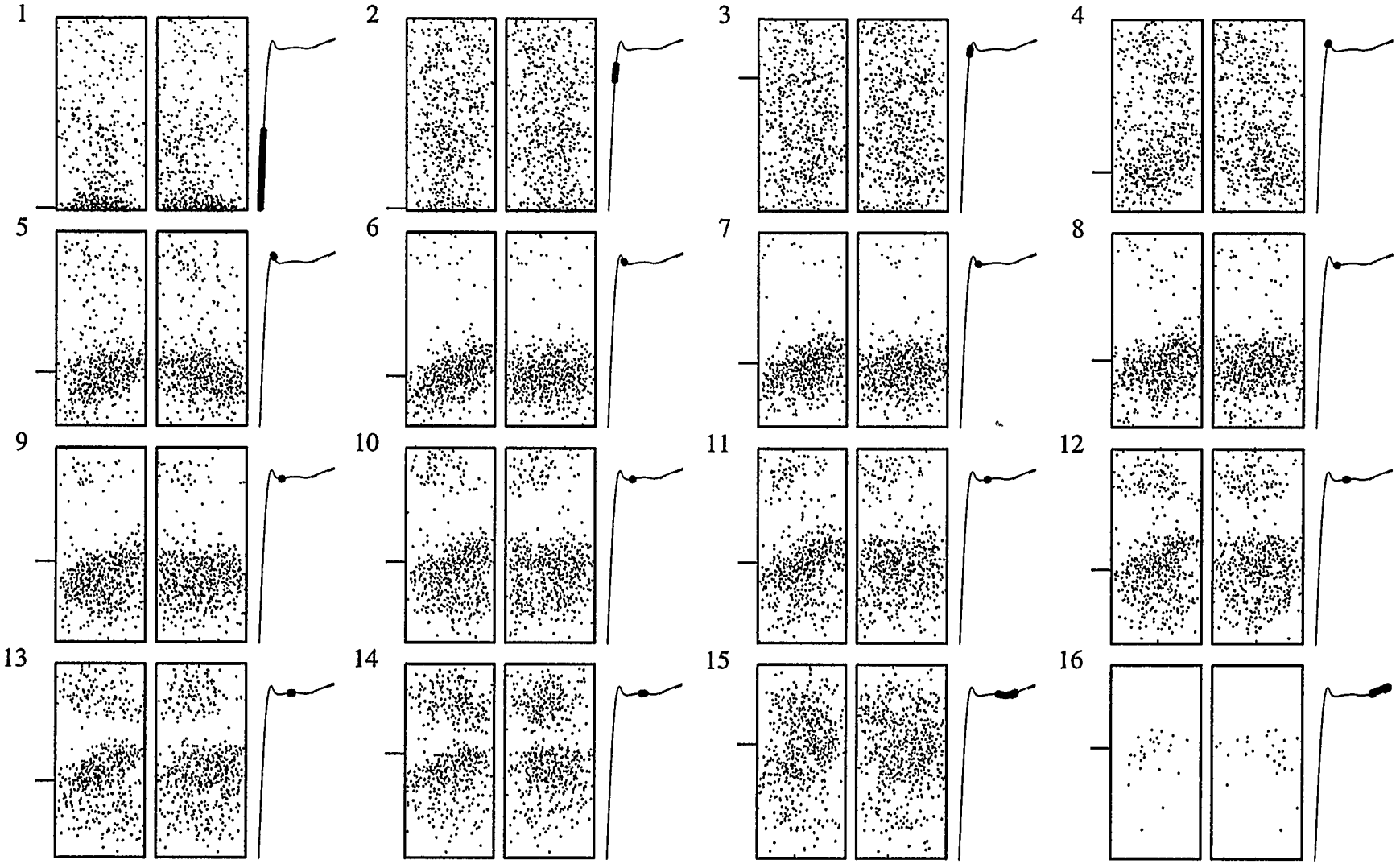

Figure 3: Orthogonal views of AE locations (•) at 16 successive stages of the test indicated by the highlighted portion of the stress-strain curve. Left and center panels of each set show all AE locations projected onto orthogonal planes parallel to the cylinder axis. Tick at left shows position of maximum AE density (Panel 3 tick is meaningless due to uniformity of distribution). Sample outline is shown as the box around the AE locations. The right hand panel displays σ_D as a function of ϵ_{11}.

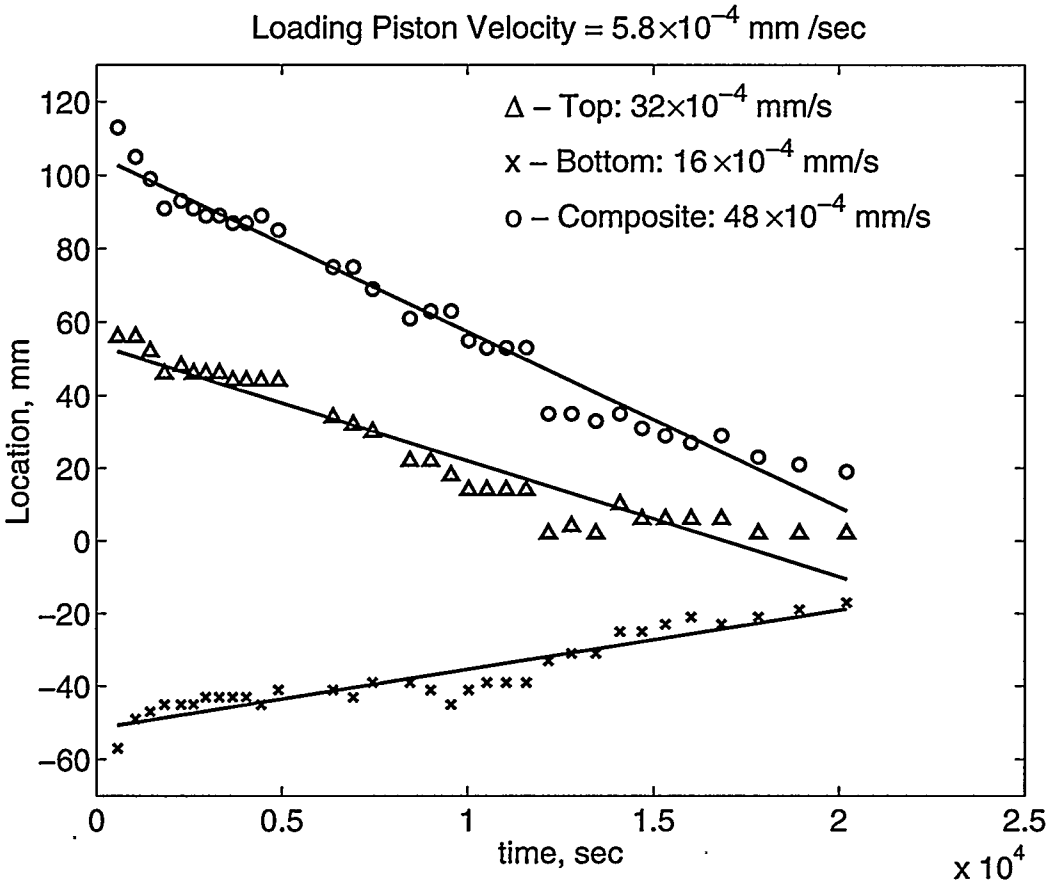

Figure 4: Location of the compaction band front plotted against time (symbols), with the best-fit velocity indicated by lines. The velocity of the loading piston was 5.8×10^{-4} mm/s. The peak stress occurred at a time between the first and second plotted points.